Physical modeling of microseismics and time reversal

Joe Wong, Hongliang Zhang, Kevin Bertram, and Kris Innanen

ABSTRACT

We have conducted two physically-modeled experiments: a microseismic survey to acquire survey data for hypocenter location through an HTI layer, and a time reversal-time study demonstrating propagation reciprocity and wave focusing. Hypocentre location in 3D is normally done using raytracing to match observed event times. In our case, raytracing requires formulas giving accurate description of anisotropic velocities through HTI media. We suggest that the Byun equations are suitable for this purpose.

To completely replicate time-reversal experiments reported in the literature, we must drive the ultrasonic transducers used as seismic sources in physical modeling with time-reversed seismic traces. At present, we can drive source transducers only with impulse functions. Therefore, we have conducted our time-reversal experiment with impulses properly delayed to enforce the main point of time-reversal, which is that multiple sources can be activated in such a way so as to focus acoustic energy at a compact zone centred about a single point. The impulsive waveforms recorded in the physically-modeled experiment can be numerically convolved with a time-reversed received signal. This procedure yields a simulation of data that would have resulted if we had actually used such a waveform to drive the sources in acquisition.

1. A MICROSEISMIC SURVEY THROUGH AN HTI LAYER

Figure 1.1 displays the geometry used for a microseismic experiment. The model consists of a flat phenolic HTI layer immersed in water. The coordinate system of the model is set up with x-axis aligned with the fast direction of the HTI layer. Receivers are on crossed and circular arrays located about 227m above the HTI layer. The angle φ between the x-axis and arm AA' of the crossed array is 27 degrees CCW. Arm BB' is orthogonal to arm AA'. The radius of the circular array is 500m. A single fixed source transducer located 100m below the bottom of the HTI layer the PVC layer represents the microseismic hypocentre. The scale factor used in the experiment is 10^4, i.e., 1mm and 0.1μs in the model represent 10m and 1ms in the real world, respectively. Simulated microseismic data were acquired by activating the source transducer with impulses.

Figure 1.2 shows microseismograms from arms AA' and BB' of the crossed receiver array. Figure 1.3 displays microseismograms from the circular array. As expected, first arrival times are least in at azimuth angles 0, 180, and 360 degrees, directions parallel to the fast direction of the HTI medium.

Location of the hypocentre requires 3D ray-tracing through the HTI layer. Thomsen (1986) and Byun et al. (1989) have published formulas that are suitable for approximating P-wave velocities through VTI and HTI media. VTI and HTI velocity anisotropy have a single axis of symmetry, with group velocities dependent on dip angle but invariant with azimuth angles about this axis. The difference between VTI and HTI is

that the axis of symmetry is in the vertical direction for VTI but is in the horizontal direction for HTI.

Kumar et al. (2004) and Casasanta et al. (2008) compared quasi-P (qP) group velocities, raypaths, and travel times from the exact treatment of VTI and from the Thomsen and Byun approximations. They showed that the Byun formulation gave better results than the Thomsen approximations in that they were closer to results derived from the exact treatment of VTI. On the basis of this, Kumar et al. (2004), Casasanta et al. (2008), and Wong (2010) chose to use the Byun approximation in devising two-point ray-bending schemes for finding travel times though media having isotropic, VTI, and HTI layers. The relevant Byun expressions are

$$V_p^{-2}(\emptyset) = a_0 + a_1 \cos^2\emptyset - a_2 \cos^4\emptyset \ , \tag{1.1}$$

$$a_0 = V_h^{-2} \ , \tag{1.2}$$

$$a_1 = 4V_{45}^{-2} - 3V_h^{-2} - V_v^{-2} \ , \tag{1.3}$$

$$a_2 = 4V_{45}^{-2} - 2V_h^{-2} - 2V_v^{-2} \ , \tag{1.4}$$

where V_0, V_{90}, and V_{45} are the group velocities in the parallel ($\emptyset$=0°), orthogonal ($\emptyset$=90°), and 45° angle directions, and $\emptyset$ is the 3D angle measured from the axis of symmetry. For geological materials, V_{90} is greater than V_0, and V_{45} is intermediate between the two. For the isotropic case, a_1 and a_2 are identically zero.

Because the receivers and source are located in water, the data from this experiment are suitable only for hypocentre location and cannot be used for source mechanism analysis. If we assume that the geometry and values of the velocity structure is fully known, the location problem will be one of determining just the coordinates (x_s, y_s, z_s, t_0) of the microseismic hypocentre given event times observed on microseismograms. This can be done either by ray tracing, or by applying time-reversal focusing. Alternatively, it can be treated as a more complex 3D problem, we treat every parameter as unknown and to be determined: the hypocenter coordinates (x_s, y_s, z_s, t_0), the velocity parameters (v_0, v_{45}, v_{90}, $\emptyset$), and the depths to top and bottom (d_1, d_2) of the HTI layer.

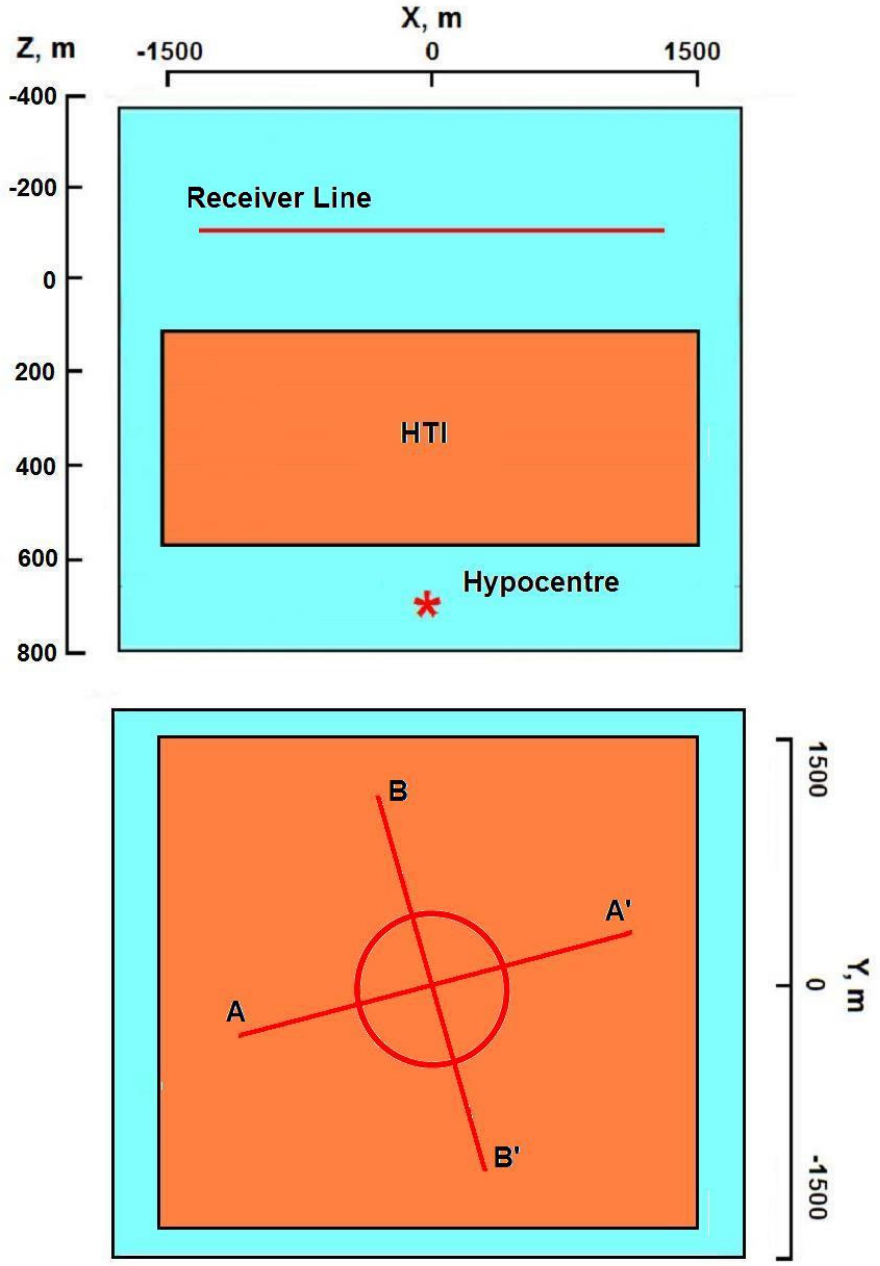

Figure 1.1: Side and plan views of model for microseismic survey. The x-axis is aligned with the fast direction of the phenolic layer. Receiver spacing along lines AA' and BB' are 44.7m. Receiver locations on the circle (radius=500m) are at angles of 0 to 360 degrees in 5 degree increments.

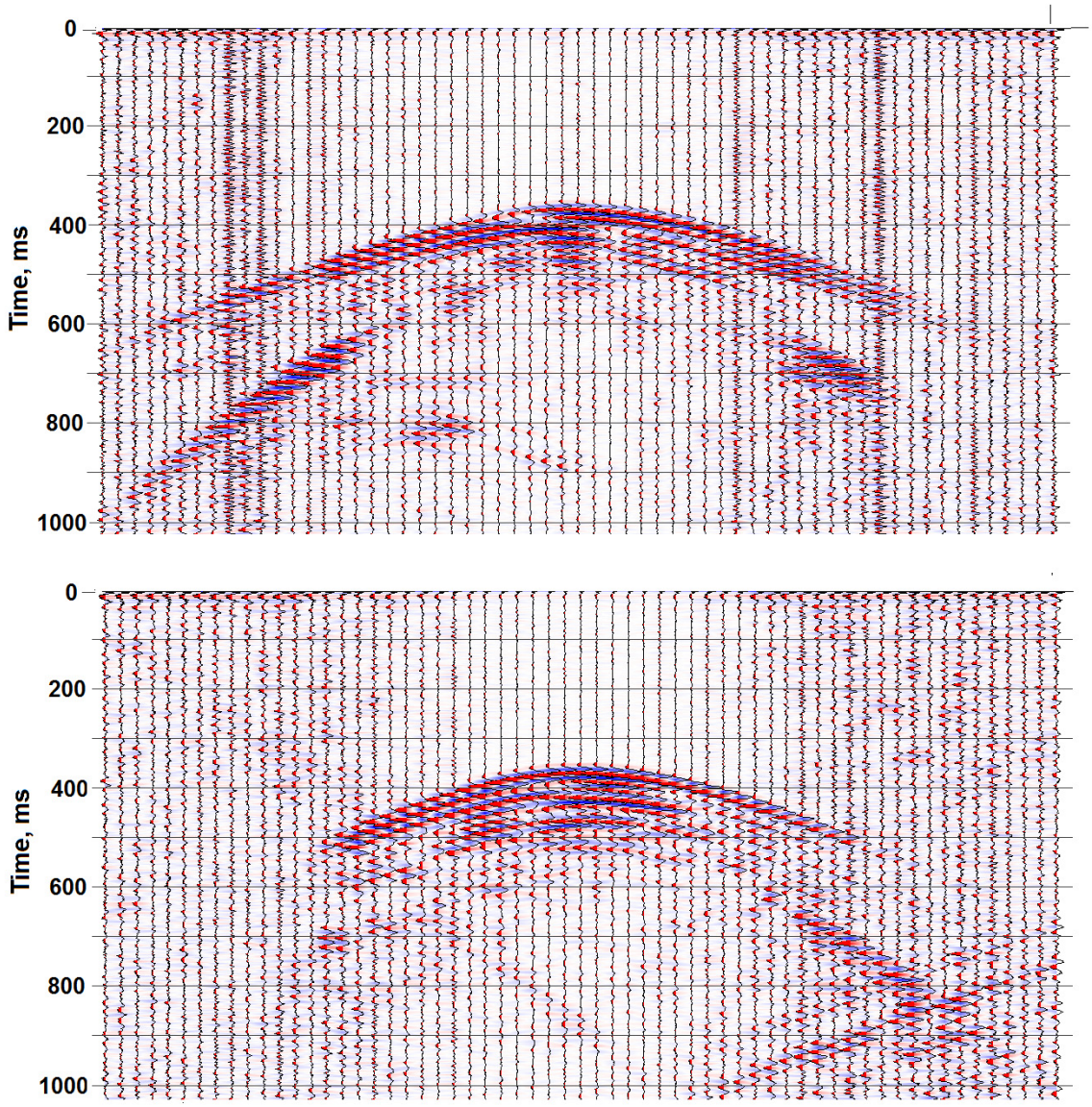

Figure 1.2: Microseismograms recorded on the crossed array. Top and bottom plots are for traces on arms AA' and BB', respectively. Spacing of receivers is 44.7m for both arms.

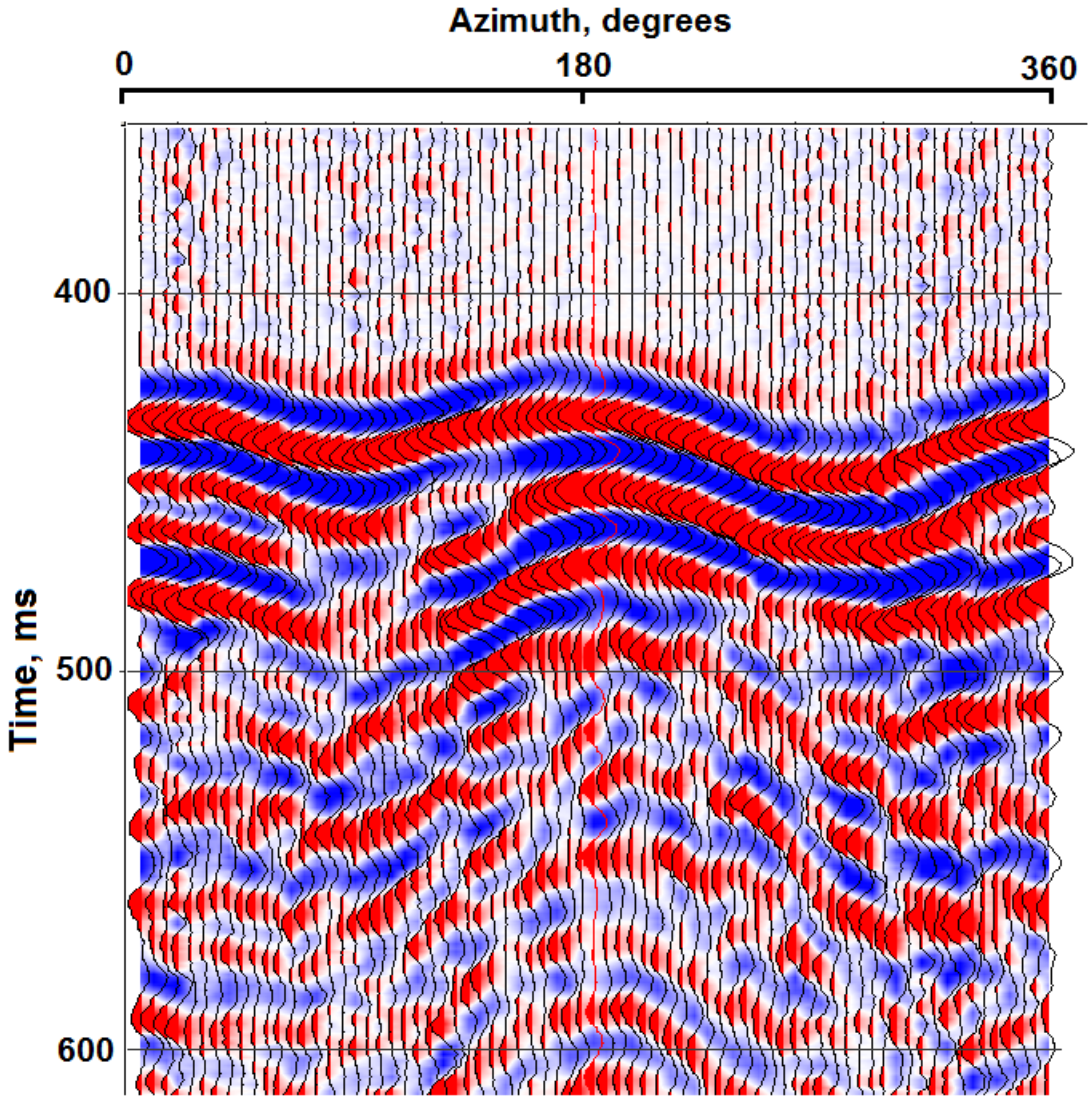

Figure 1.3: Microseismograms recorded on the circular receiver line. Minimum arrival times are evident at azimuth angles of 0, 180, and 360 degrees.

2. TIME REVERSAL EXPERIMENTS

We have conducted a physical modeling experiment on time reversal. Time reversal is an interesting idea based on the principle of reciprocity in wave propagation. Given multiple receivers and a single source in an arbitrary linear acoustic or elastic medium, ultrasonic energy can be focused at that source position if all the receivers are simultaneously excited as sources by their respective received signals reversed in time. In its simplest manifestation, time reversal involves first recording ultrasonic data with a source with many receivers. Then the recorded waveforms are windowed in time to include the most energetic arrivals and reversed in time. Finally, the reversed waveforms are used to drive the multiple receivers simultaneously. Reciprocity guarantees that the wave energy transmitted from the multiple receiver positions will focus at the location of the original source point.

Fink (1992) has reviewed time reversal in the context of lithotripsy (breakage of kidney stones using focused ultrasonic energy). A patient is given an ultrasonic scan using multiple receivers (ultrasonic transducers can be used interchangeably as receivers and sources). The received waveforms are edited to contain primarily the diffracted arrivals from a kidney stone (which then can be considered as the "source"). Then transmitting the time-reversed edited waveforms using the receivers as sources (without moving their locations) will focus acoustic at the original diffraction point, i.e., the kidney stone. The focused energy would be enough to shatter the stone if enough receivers are used as reversed sources.

In geophysics, Lellouch and Landa (2018) and Landa et al. (2019) have referred to the relationship of time reversal to reverse-time migration, its potential application to microseismic hypocentre location, and as an alternative to ray-tracing-based tomography and full-wave inversion for finding velocity structure. Landa et al. (2019) and Landa and Shustak (2019) have described a three-step geophysical experiment conducted in a cave that confirmed the focusing capability of time reversal.

1. A hammer acting on the top surface of the cave produced seismograms recorded on the ground surface 30m above. This is the forward survey.

2. They then carried out a reverse survey. A controllable source based on a LSM (linear synchronized motor; Noorlandt, 1994) acted sequentially at the 48 received positions produced vibrations replicating the time-reversed received waveforms. For each controlled source, seismograms were recorded at an array of 12 receivers glued to the top of the cave. One such receiver occupied the position where the source was located in step 1. The forward survey receivers thus reversed in function becoming sources driven by the respective time-reversed received signals are called the time-reversal mirror (TRM; Fink, 1994).

3. The received seismograms at each receiver from the reverse survey were summed and plotted. The plots confirmed focusing at the original source point.

In the physical modeling laboratory, we have carried out a similar experiment. We set up the model geometry shown on Figure 2.1, and recorded impulsive seismograms using

a single piezopin source shooting through a velocity structure from below into a piezopin receiver located along a line above the structure. This forward survey produced the seismograms shown on Figure 2.2(a); the time-reversed version of the forward survey seismograms is plotted on Figure 2.2(b).

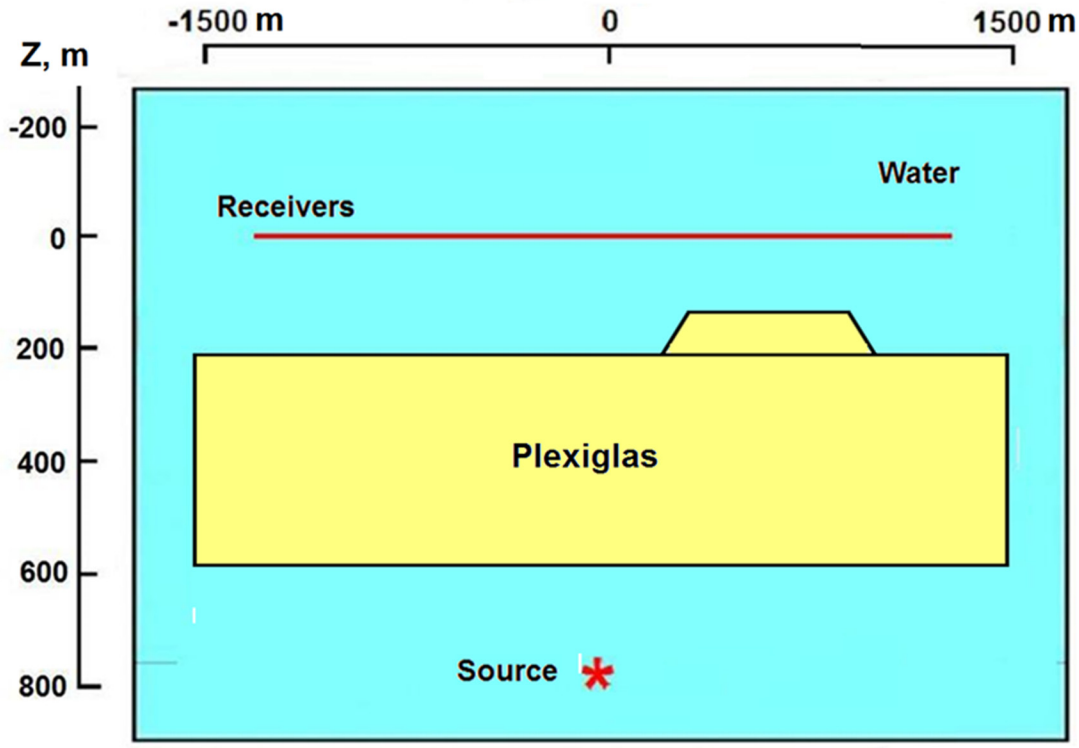

Figure 2.1: Schematic of physical model for the time reversal experiment.

The reverse survey (second part of the experiment) required locating the above-structure transducer at a subset of the receiver positions above the velocity structure and activating it as a source. Eleven chosen positions and the associated seismograms are shown on Figure 2.3, as well as the associated received waveforms. At each chosen position, the receiver-switched-to-source should be driven by the associated signals shown on Figure 2.2(b). We do not yet have the capability to electronically drive source transducers with waveforms equal to the time-reversed received waveforms. Therefore we opted to activate each reversed source with impulses at delay times determined by the time picks shown on Figure 2.3. As each switched source was activated, impulsive seismograms were recorded using the original source transducer as a receiver and moving it along a line below the Plexiglas structure, taking care that traces were recorded at the original source location.

Eleven such impulsive common-source gathers were acquired in our reverse survey; three of these are shown on Figure 2.4(a).

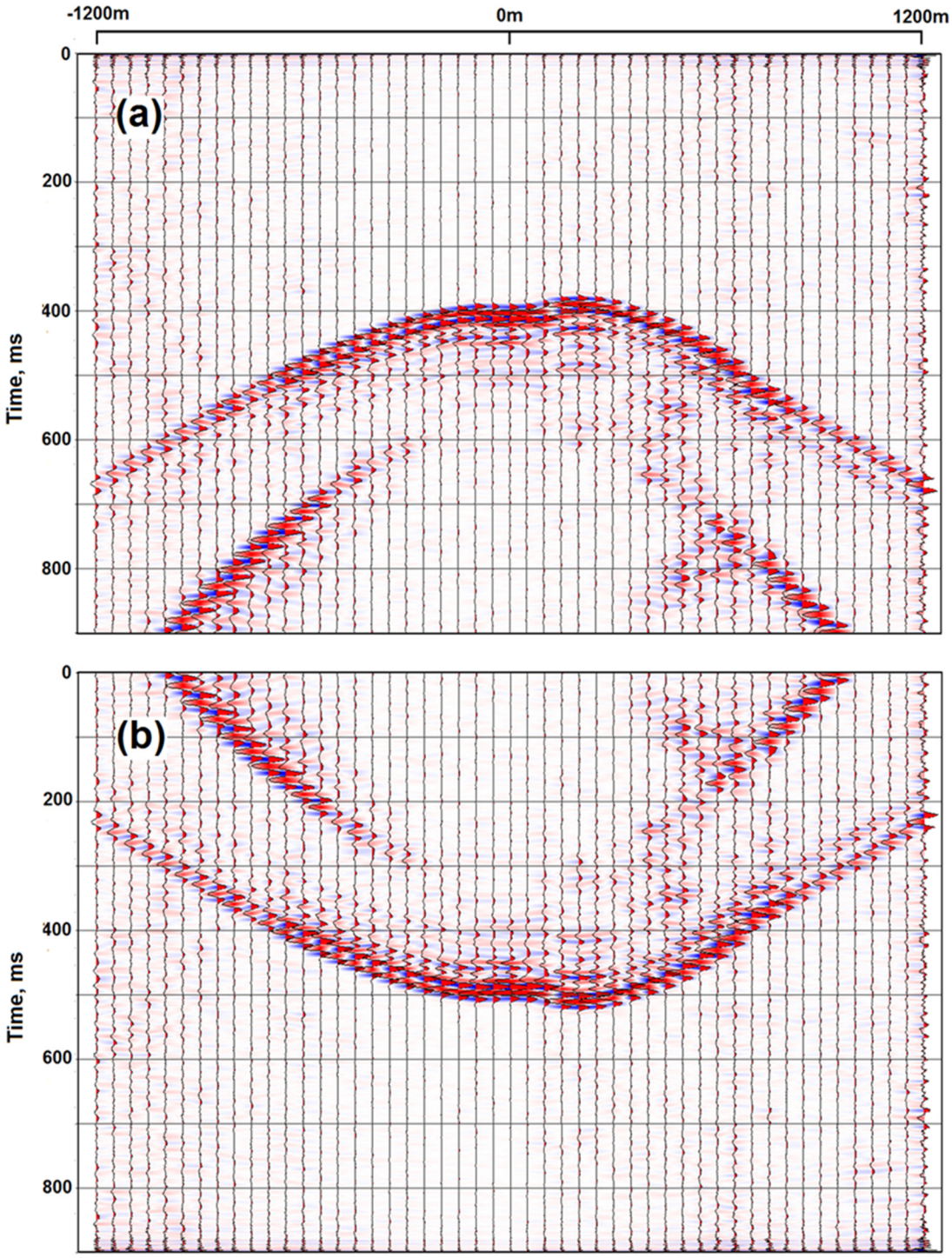

Figure 2.2: (a) Physical model seismograms acquired in the forward survey, with a single subsurface source shooting through the velocity structure to surface receivers. (b) Mirrored and time-reversed traces.

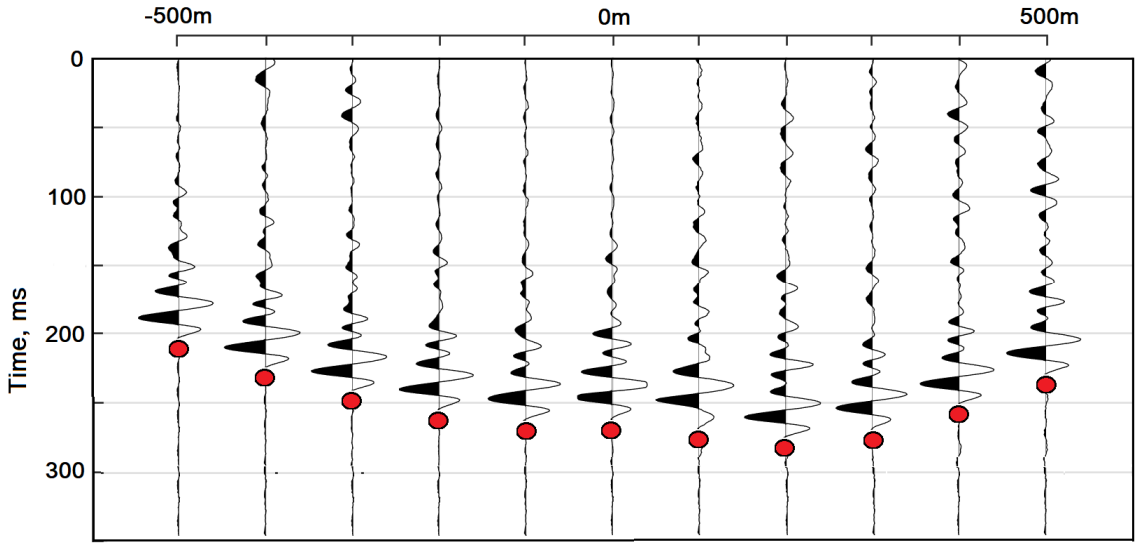

Figure 2.3: Selected windowed and reversed waveforms obtained from the forward survey. The positions shown are the eleven source positions for the reverse survey. Red dots indicate the time picks used to determine relative time delays for firing the switched sources.

Figure 2.4(b) displays the result of numerically convolving the traces on Figure 2.4(a) with the reversed waveform located at position 0m on Figure 2.3. This procedure simulates the physical action of electronically activating the source with the reversed waveforms on Figure 2.3. The result is data that would have resulted if the switched sources had been activated electronically with the reversed waveforms. Comparing, Figures 2.4(a) and 2.4(b), we see that convolution has produced fairly minor differences in the signal shapes. The major observable effect of convolving with the windowed reversed signals is that the first arrivals are delayed.

The final step in our time reversal experiment is to add together the eleven gathers recorded with reversed impulsive sources. The result is displayed on Figure 2.5(a). There is good focusing at position 0m on the lower receiver line (location of the source in the forward survey). Firing the sources impulsively with properly set relative delays (determined by the time picks shown on Figure 2.3) ensures that the first arrival energy from the 11 sources focuses at the receiver position corresponding to the source position in the forward survey. We have used only eleven reversed sources in the acquisition; the focusing should improve if more reversed sources are used.

To complete the experiment, we also summed eleven reversed gathers obtained by numerical convolution of impulsive source gathers with a reversed received signal source waveform. For convenience, we have used windowed time-reversed received signals to do the convolution in this demonstration, but windowing is not necessary. The one requirement is that the reversed signal must contain the coda from strong events. Driving the source transducers with unwindowed reversed received signals requires no time-picking to find the proper delays for impulsive firing.

SUMMARY AND CONCLUSION

We have completed a microseismic physical modeling survey acquiring data intended to simulate a fairly complicated hypocentre location problem. Microseismograms were recorded on surface receivers with a single source representing a hypocentre beneath an HTI layer. Receivers were positioned on a crossed linear array and on a circular array. The complication in locating the hypocentre in 3D arises from the need to ray-trace through the HTI material. For the ray-tracing, we suggest that the Byun equations for approximating HTI velocities be used as a better alternative to the Thomsen equations.

We also have conducted a time reversal experiment, in which we recorded data demonstrating the concept of a time-reversal mirror (TRM). In essence, time reversal involves a forward survey recording data with a set of receivers and a single source through an arbitrary non-attenuating velocity field. In the reverse survey, the received seismograms are time-reversed, the receivers are changed to sources, and the single source becomes a receiver. Simultaneously activating the receivers-switched-to-sources with the time-reversed received traces, and recording with the source-switched-to-receiver yields common source gathers whose sum shows the energies from the individual sources focusing in a zone centred about the forward survey source location. Although we were not able to drive our sources with high-voltage versions of the time-reversed seismograms, we were able to replicate the focusing by driving the switched receivers with impulses delayed according to the first-arrival times on the original received seismograms. Time reversal is a consequence of reciprocity in wave propagation. Numerical convolution with a time-reversed signal from our forward survey of the impulsive seismograms recorded in our reversed survey indicates that the convolution procedure does not affect focusing.

ACKNOWLEDGEMENTS

We thank the sponsors of CREWES for continued support. This work was funded by CREWES industrial sponsors, NSERC (Natural Science and Engineering Research Council of Canada) through the grant CRDPJ 461179-13, and in part by the Canada First Research Excellence Fund.

REFERENCES

Byun, B.S., Corrigan, D., and Gaider, J.E., 1989. Anisotropic velocity analysis for lithology discrimination: Geophysics, **54**, 1566-1574.

Casasanta, L., Drufucca, G., Di Milano, P., Andreoletti, C., and Panizzardi, J., 2008. 3D anisotropic ray tracing by raypath optimization: Expanded Abstr., 78th Ann. Internat. Mtg., Soc. Expl. Geophys., Expanded Abstracts.

Fink, M., 1992. Time reversal of ultrasonic fields. Part I- Basic principles: IEEE Transactions on Ultrasonic, Ferroelectrics, and Frequency Control, **39**, 555–566.

Kumar, D., Sen, M.K., and Ferguson, R.J., 2004. Traveltime calculation and prestack depth migration in tilted transversely isotropic media: Geophysics, **69**, 37-44.

Landa, E., A., Yurman, and R., Jenneskens, 2019. Seismic time reversal mirror experiment: First Break, **37**, 41–45,

Landa, E., A and Shustak, M., 2019. Time reversal in seismic: 89th Ann. Internat. Mtg., Soc. Expl. Geophys., Expanded Abstracts, 4735-4739.

Lellouch, A., and E., Landa, 2018, Seismic velocity estimation using time-reversal focusing: Geophysics, **83**, no 4, U43–U50,

Noorlandt, R., G., Drijkoningen, J., Dams, and R., Jenneskens, 2015. A seismic vertical vibrator driven by linear synchronous motors: Geophysics: **80**, no. 2, EN57–EN67.

Thomsen, L., 1986. Weak elastic anisotropy, Geophysics: **51**, 1954-1966.

Wong, J., 2010. Fermat's principle and ray tracing through anisotropic layered media: CREWES Research Report, **22**, 88.1-88.8.

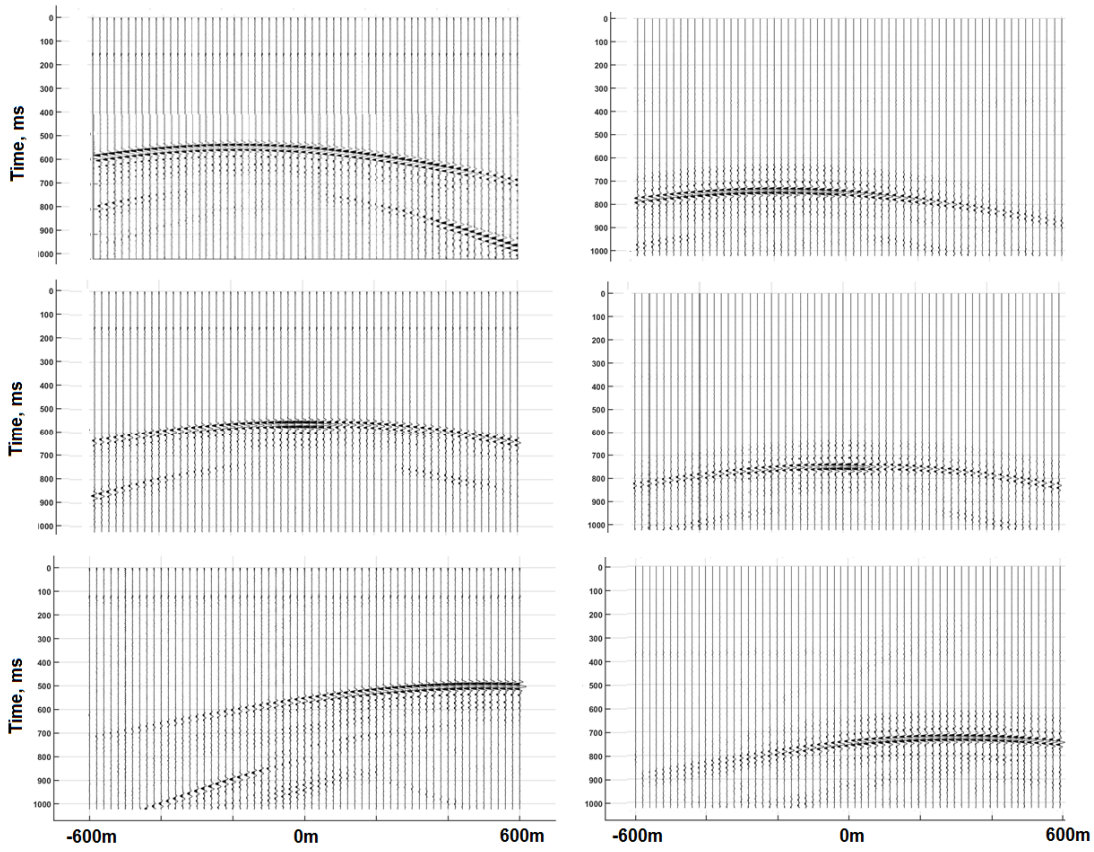

Figure 2.4: Reverse survey data. (a) Common-source gather of impulsive seismograms for the switched source located at -200m, 0m, and 500m along the line above the Plexiglas structure. (b) Gather of seismograms that would have resulted if the source had been driven electronically by a reversed signal from Figure 3, simulated by numerically convolving seismograms in (a) by the reversed signal at position 0m on Figure 3.

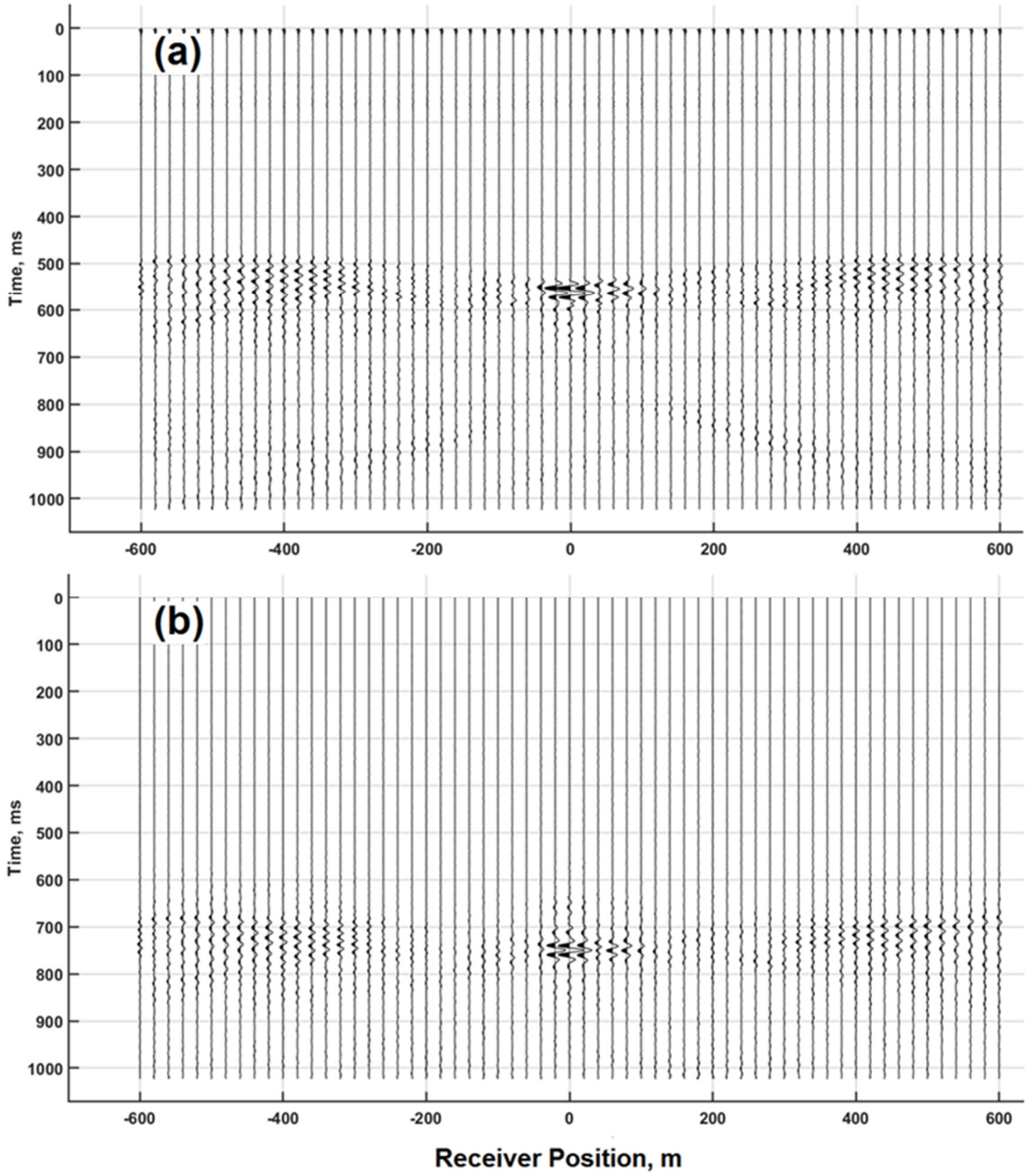

Figure 2.5: Reverse survey result. (a) Summation of eleven common-source gathers recorded with reversed impulsive sources at positions -500m to 500m with spacing of 100m.There is good focusing of energy at the original source location below the velocity structure. (b) Summation of eleven simulated common-source gathers, the result of convolving the eleven impulsive gathers with a reversed signal from Figure 3. The use of reversed signals to generate time reversal data does not appear to affect spatial focusing, although focus time has been shifted to later times by the convolution procedure.